79.

[redacted]

MSFC

MTP-AERO-62-29
March 20, 1962

36p

X63 15957

Code 2C

GEORGE C. MARSHALL SPACE FLIGHT CENTER

HUNTSVILLE, ALABAMA

CLASSIFICATION CHANGE

TO - UNCLASSIFIED ~~[illegible]~~

By authority of T.D. No. 74-126

Changed by [illegible] Date 1/11/74

NASA TMX 50497

PROPELLANT SLOSHING PROBLEMS OF SATURN TEST FLIGHT SA-1 (U)

By

Helmut F. Bauer

[redacted]

NASA

[redacted]

NATIONAL AERONAUTICS AND SPACE ADMINISTRATION

(NASA-TM-X-50497) PROPELLANT SLOSHING PROBLEMS OF SATURN TEST FLIGHT SA-1 (NASA) 36 p

N74-71623

Unclas
00/99 29882

GEORGE C. MARSHALL SPACE FLIGHT CENTER

MTP-AERO-62-29

PROPELLANT SLOSHING PROBLEMS OF SATURN TEST FLIGHT SA-1 (U)

By Helmut F. Bauer

(U) ABSTRACT 15957

This paper presents propellant sloshing problems and their solutions encountered in the development of the Saturn space vehicle with clustered tanks. Attention is given to the regular sloshing, its description by an equivalent mechanical model, laboratory model tests in which the effectiveness of baffle width, location, and geometry can be determined, and to the vortex problem of emptying containers. The interconnection of clustered tanks complicates the problem by presenting a new U-tube mode. To insure vehicle stability, the propellant in the tanks should have proper damping, the value of which can be determined by stability boundaries. The over-all stability, with the inclusion of propellant sloshing, elastic effects of the structure, and the control system has also been investigated. This report also compares test flight results of SA-1 with these previously obtained theoretical results.

To improve sloshing stability at the end of the powered flight of future Saturn Vehicles, a set of accordion baffles will be included for all remaining Block I Vehicles. These baffles will cover the last three stiffener rings in the Lox and fuel tanks.

Uncl. AUTHOR

[redacted]

GEORGE C. MARSHALL SPACE FLIGHT CENTER

MTP-AERO-62-29

March 20, 1962

PROPELLANT SLOSHING PROBLEMS OF SATURN TEST FLIGHT SA-1 (U)

by

Helmut F. Bauer

AEROBALLISTICS DIVISION

[redacted]

(U) TABLE OF CONTENTS

(U) LIST OF ILLUSTRATIONS

(U) LIST OF ILLUSTRATIONS (Cont'd)

(U) DEFINITION OF SYMBOLS

$a = \frac{d}{2}$	Tank radius
h	Liquid height
g	Longitudinal acceleration
ω_n (ω_s)	Natural circular frequency of liquid
ϵ_n	Zeros of $J_1'(\epsilon)$
J_1	Bessel function of first kind and first order
x_o	Excitation amplitude in x-direction
θ_o	Excitation amplitude about y-axis
ρ	Liquid density
F	Liquid force
k_n	Spring constant of n^{th} sloshing mode
m_n	Mass of the n^{th} sloshing mode
m_o	Fixed nonsloshing mass
m	Total liquid mass
h_o	Distance of fixed mass from center of gravity of undisturbed liquid
h_n	Distance of n^{th} sloshing mass from center of gravity of undisturbed liquid, or distance of suspension point of n^{th} sloshing mode pendulum
ω	Forced circular frequency
t	Time
c_n	Damper constant of n^{th} sloshing mode

(U) DEFINITION OF SYMBOLS - CONTINUED

γ_n (γ_s)	Damping factor of n^{th} sloshing mode
I_o	Moment of inertia of fixed mass about its center of gravity
η_n	Displacement of n^{th} sloshing mass relative to tank wall
I_1	Moment of inertia of disc
I_{rigid}	Moment of inertia of solidified liquid
c_1	Damper constant of disc dashpot
$\frac{\mu}{\rho} = \nu$	Kinematic viscosity
w	Width of baffle
d	Depth of baffle below free liquid surface
$s = \sigma + i\omega$	Complex frequency
I_{eff}	Moment of inertia of the vehicle about the center of gravity
k^2	Square of the radius of gyration
a_o, a_1	Gain values of attitude control system
μ	Ratio of sloshing mass to total vehicle mass
ω_c	Control frequency (radians/sec)
ζ_c	Control damping
x_{CR}	Location of center of instantaneous rotation

GEORGE C. MARSHALL SPACE FLIGHT CENTER

MTP-AERO-62-29

PROPELLANT SLOSHING PROBLEMS OF SATURN TEST FLIGHT SA-1 (U)

By Helmut F. Bauer

SECTION I. (U) SUMMARY

This paper presents propellant sloshing problems and their solutions encountered in the development of the Saturn space vehicle with clustered tanks. Attention is given to the regular sloshing, its description by an equivalent mechanical model, laboratory model tests in which the effectiveness of baffle width, location, and geometry can be determined, and to the vortex problem of emptying containers. The interconnection of clustered tanks complicates the problem by presenting a new U-tube mode. To insure vehicle stability, the propellant in the tanks should have proper damping, the value of which can be determined by stability boundaries. The over-all stability with the inclusion of propellant sloshing, elastic effects of the structure, and the control system has also been investigated. This report also compares test flight results of SA-1 with these previously obtained theoretical results.

SECTION II. (U) INTRODUCTION

Liquid in a partially-filled container has a strong tendency to "slosh" about, even under the slightest disturbance. Propellant sloshing in the tanks of a space vehicle will seriously affect the performance and stability of the vehicle, sometimes causing complete failure. That the influence of propellant sloshing upon stability is an acute problem is obvious, since, for most vehicles at launch, more than 90 percent of the total weight is represented by liquid propellants. Now, if the natural frequencies of the propellant in the tanks are close to the control frequency, or to the lower modes of elastic vibration, say the fundamental body-bending mode or to the natural frequency of a control sensor, then the problem becomes extremely involved. It is for this reason that, for a realistic dynamic stability and control analysis, the effect of the oscillating propellant has to be considered.

The purposes of this study were to find solutions to problems of propellant sloshing in space vehicles of the clustered-tank variety and to determine the amount of tank baffling necessary to insure vehicle stability. Some of the problems peculiar to liquid propellants are discussed with respect to the Saturn vehicle. (FIG. 1)

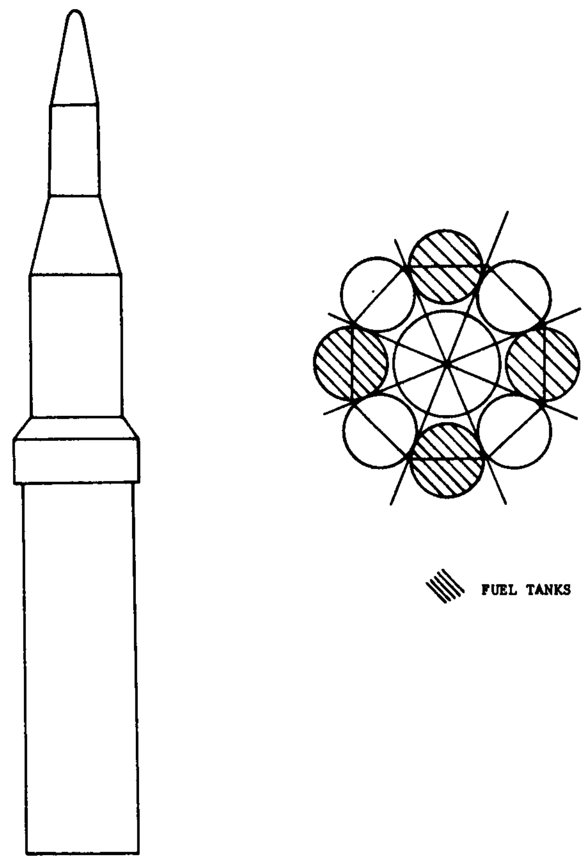

FIGURE 1. (U) SATURN SA-1 AND BOOSTER TANK ARRANGEMENT

A cluster of a Jupiter tank with eight Redstone tanks was selected for the Saturn vehicle. This approach allowed use of the existing tools and experience and reduced the cost and development time. It also proved to be beneficial from the standpoint of the influence of propellant sloshing upon stability.

The influence of these propellant oscillations depends on the amount of oscillating propellant, as well as the kind of control system involved, and its gain values.

The effect of the elastic structure upon propellant sloshing is also becoming more pronounced since a long vehicle the size of the Saturn exhibits much lower bending frequencies than those encountered in previous missiles.

SECTION III. (C) DISCUSSION

A. (U) THEORY.

The mathematical theory of the liquid oscillation in a cylindrical container which is based on a linearized potential theory treating the propellant as incompressible, irrotational and nonviscous (Ref. 12). The Eigen values obtained from the free oscillation analysis are:

$$\omega_n^2 = \frac{g}{a}\,\epsilon_n \tanh\left(\epsilon_n \frac{h}{a}\right), \qquad n = 0,1,2,\ldots. \tag{1}$$

where ϵ_n is a root of $J_1'(\epsilon) = 0$ and has the values:

$\epsilon_o \approx 1.84$

$\epsilon_1 \approx 5.33$

$\epsilon_3 \approx 8.53.$

The natural frequency of the propellant is therefore:

$$f_n = \frac{1}{2\pi}\sqrt{\frac{g}{a}\,\epsilon_n \tanh\left(\epsilon_n \frac{h}{a}\right)}. \tag{2}$$

It can be seen from this frequency equation that the natural frequency of the propellant increases with the square root of the longitudinal acceleration, g, and is indirectly proportional to the square root of the tank diameter. For constant tank dimensions and longitudinal acceleration, most of the change in frequency occurs for shallow propellant depths, i.e., for a fluid height of less than one tank diameter for the first mode and even less for higher modes. Due to increasing longitudinal acceleration, the natural frequency of the propellant versus flight time increases (FIG. 2). Only shortly before burn-out does the influence of fluid height overcome the influence of the acceleration, g, and decrease the frequency again.

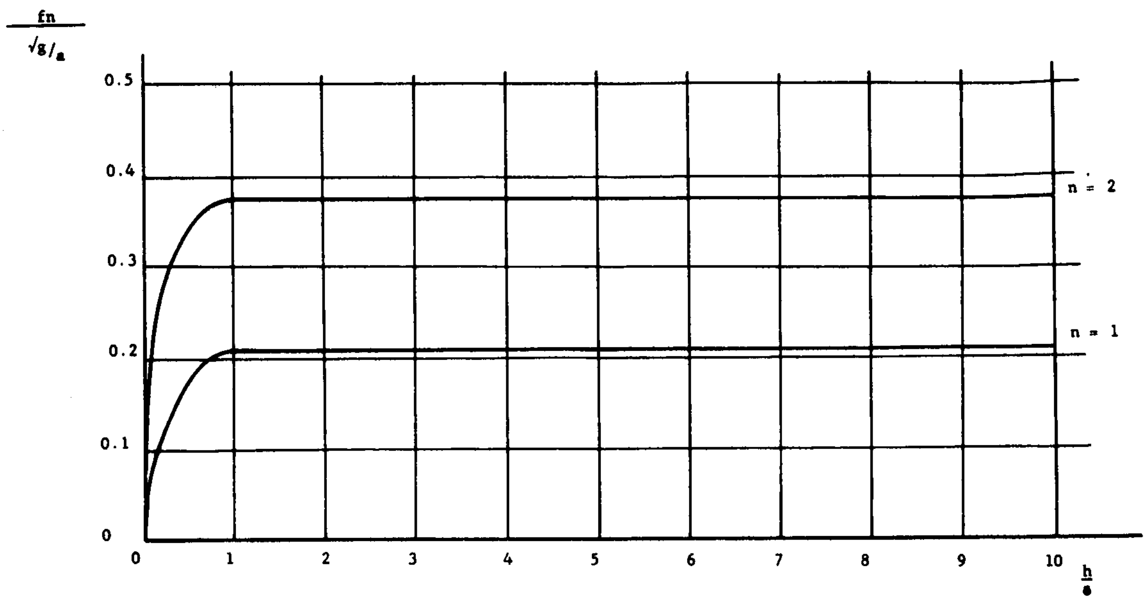

FIGURE 2. (U) NATURAL FREQUENCIES FOR CIRCULAR CYLINDRICAL CONTAINER

It can be seen that the natural frequency in the center tank (105-inch diameter tank) ranges versus flight time from 0.70 cps to 1.14 cps, while that of the outer tanks(70-inch diameter tanks) increases from 0.86 cps at lift-off to a maximum of 1.41 cps. FIGURE 3

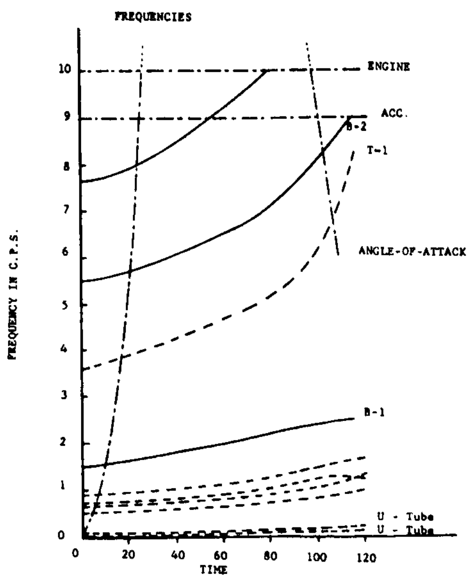

FIGURE 3. (U) FREQUENCY SPECTRUM OF SATURN

exhibits the frequency spectrum. The control frequency is about 0.3 cps and is not indicated in the figure. Noted with B-1, B-2, and B-3 are the bending frequencies of the first, second, and third bending mode, while T-1 represents the frequency of the first torsional mode. Accelerometer frequency, represented by ACC., was not used in the SA-1 flight.

The flow field of the liquid with free fluid surface in a cylindrical tank with a circular cross section and a flat tank bottom, due to forced oscillation of the tank, can be obtained as a solution of the Laplace equation and the appropriate linearized boundary conditions. The result, however, exhibits singularities at the resonance of the liquid. FIGURE 4 shows the magnification factor of the force of the liquid in a circular cylinder for translation and rotational excitations.

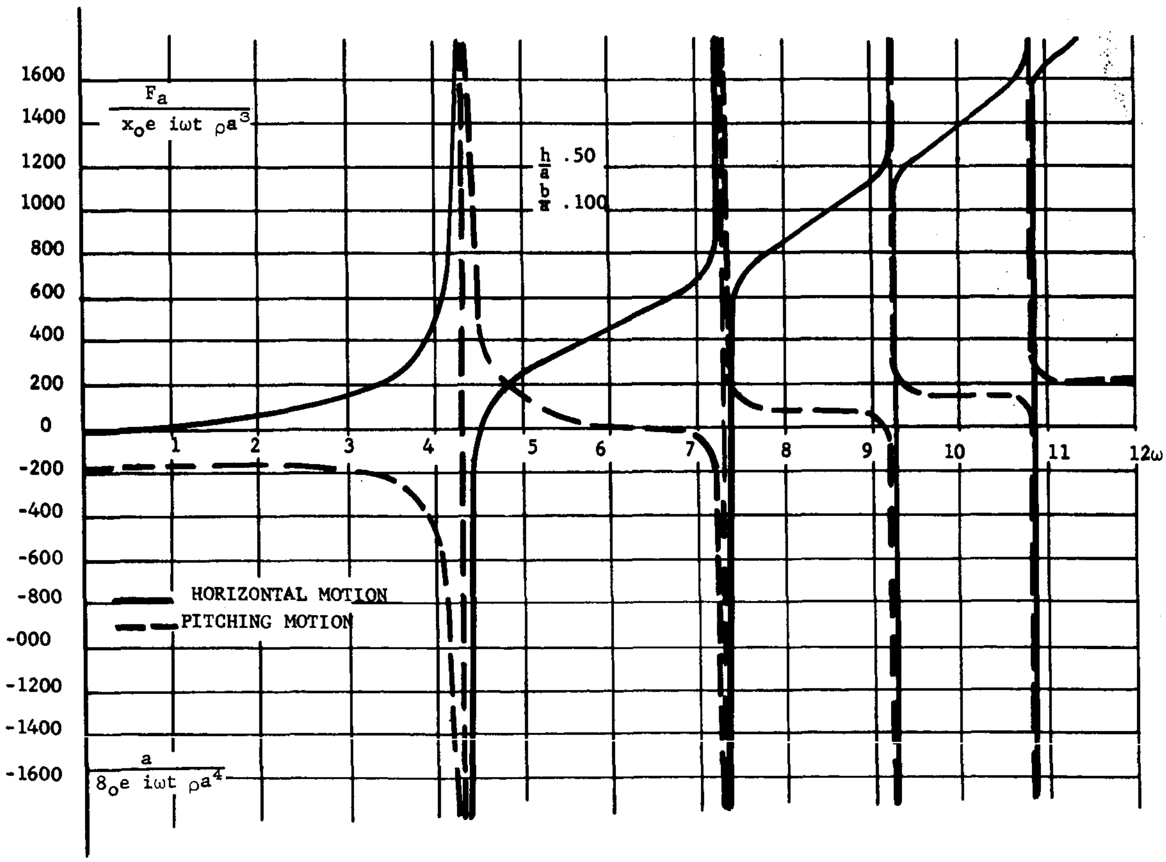

FIGURE 4. (U) MAGNIFICATION FACTOR OF THE LIQUID FORCE IN A CIRCULAR CYLINDRICAL TANK (UNDAMPED)

The theory does not yield the answer of the liquid motions for large amplitudes which occur near or at resonance. But the reaction of the propellant near resonance has there the critical influence upon stability. Furthermore, it does not give an answer for the inclusion of mechanical suppression devices, or baffles, of one type or another. These baffles, or at least stiffener rings, are almost universally used in the liquid propellant tanks of missiles. Thus, the magnitude of forces and torques from the liquid upon the vehicle is reduced. This means that, due to the complexity of the fluid flow behavior, a mathematical treatment is impossible; therefore, recourse must be made to potential theory with smooth tank walls and experimental investigations. From these, the response of the liquid caused by forced excitation can be obtained; therefore, damping can be determined. Since the forced-damped fluid oscillations retain their amplitude - i.e., they are periodic oscillations with some nonlinear damping - a method of approximating the damping of the motion can be employed by introducing equivalent linear damping the value of which will be obtained by experiments (FIG. 5).

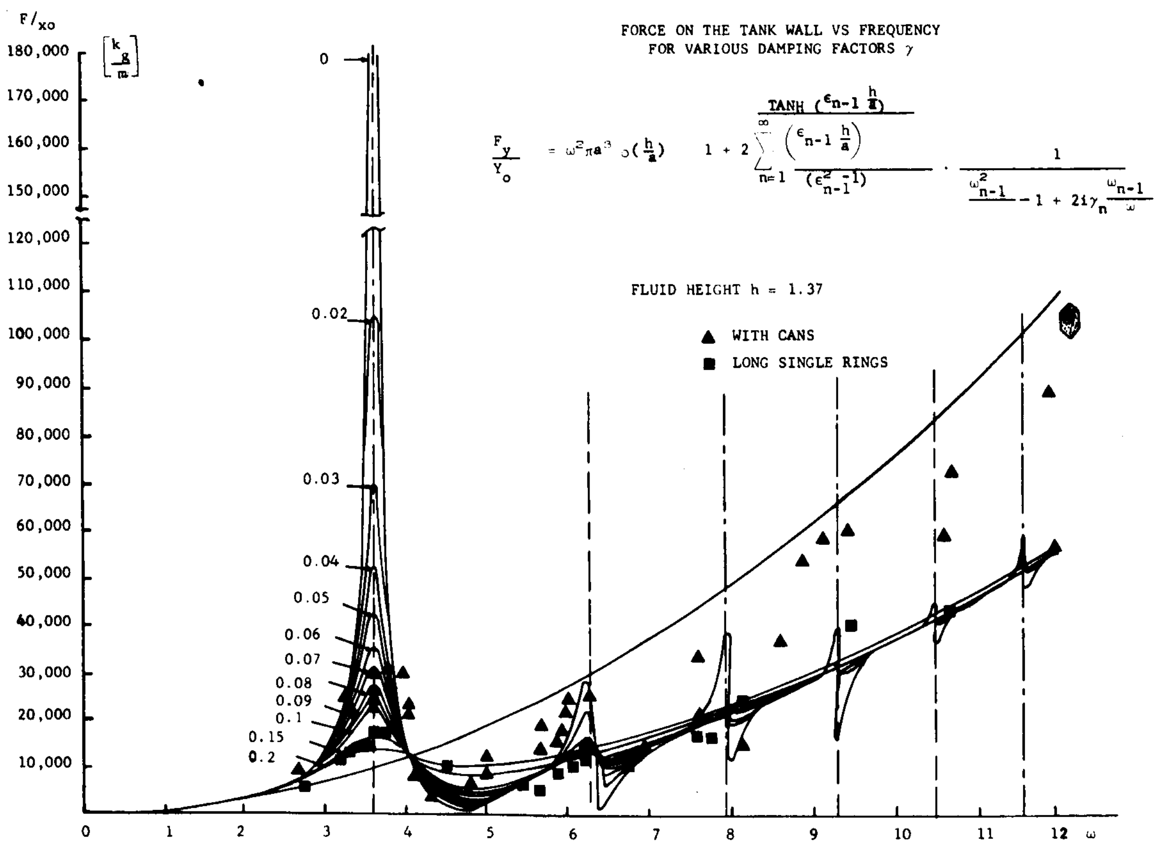

FIGURE 5. (U) MAGNIFICATION FACTOR OF THE LIQUID FORCE IN A CIRCULAR CYLINDRICAL TANK (DAMPED)

B. (U) MECHANICAL MODEL.

A mechanical model consisting of masses and springs or pendulums describes the motion of the liquid and aids the introduction of linear-equivalent damping into the fluid dynamics results. Each sloshing mode is represented by a mechanical one-degree-of-freedom system in the form of a linear mass-spring system (FIG. 6).

COORDINATES AND MODEL

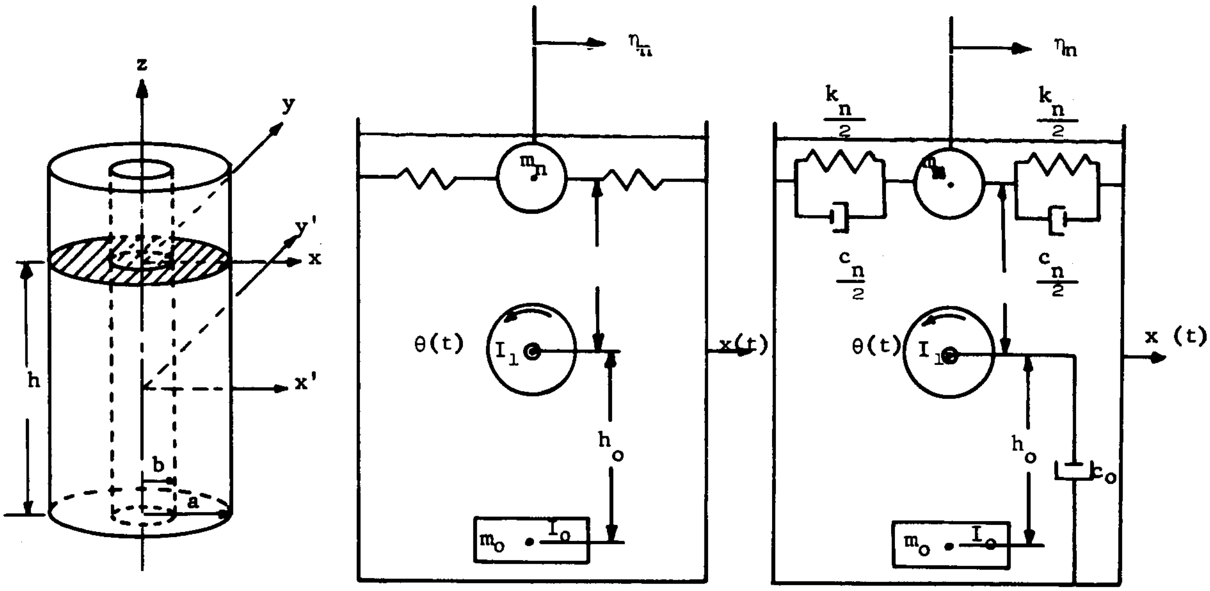

WITHOUT DAMPING

WITH DAMPING

FIGURE 6. (U) MECHANICAL MODEL

Once the damping is introduced, the family of theoretical response curves can be compared with the measured values for various damping devices; a damping factor can thus be obtained (Ref. 3).

The mechanical model consists of a fixed mass, m_o, with a moment of inertia, I_o, which represents the part of the liquid that does not perform any sloshing motion. It furthermore consists of the sloshing masses, m_n, for each mode, which are attached with springs, k_n, to the tank wall.

The locations of these masses from the origin are noted by h_n and h_o. The spring constants are chosen so that the ratio with the sloshing mass represents the square of the natural circular frequency:

$$\frac{k_n}{m_n} = \omega_n^2. \qquad (3)$$

At the center of gravity of the undisturbed liquid, a massless disc is frictionlessly attached and is connected with a dashpot to the tank bottom. The disc has the purpose of taking into account that not all the liquid is participating in the pitching motion of the tank. Tank geometry, viscosity, and the amount of baffles in the tank determine the damping coefficient, c_o, and the moment of inertia, I_1, of the disc. For potential flow, I_1 can be obtained analytically and is

$$I_1 = I_{rigid} - I_{liquid} \qquad (4)$$

where I_{liquid} is the moment of inertia of the liquid with sloshing completely suppressed (lid on surface).

$$I_{liquid} = m_o^2 \quad \frac{1}{12}\left(\frac{h}{a}\right)^2 + \frac{1}{4} - 8 \sum_{n=1}^{\infty} \frac{\left[1 - \dfrac{2}{\epsilon_n \frac{h}{a}} \tanh\left(\dfrac{\epsilon_n}{2} \dfrac{h}{a}\right)\right]}{\epsilon_n^2 \; (\epsilon_n^2 - 1)}$$

Here the first two terms represent the moment of inertia of the liquid if it were considered rigid.

These values are substituted for the liquid mass, m. The mechanical values m_o and m_n are:

$$m = m_o + \sum_{n=1}^{\infty} m_n.$$

Comparing the results of the analysis of the ideal liquid with those of the mechanical model finally presents the values of the sloshing masses, m_n, their distances, h_n, and the values m_o, I_o, h_o, etc. It is

$$m_n = m \frac{2 \tanh\left(\epsilon_n \frac{h}{a}\right)}{\left(\epsilon_n \frac{h}{a}\right)\left(\epsilon_n^2 - 1\right)}, \; I_o = I_{rigid} - I_1 - m_o h_o^2 - \sum_{n=1} m_n h_n^2 \qquad (5)$$

$$h_n = \frac{h}{2}\left[1 - \frac{4}{\epsilon_n \frac{h}{a}} \tanh\left(\frac{\epsilon_n}{2}\frac{h}{a}\right)\right] \text{(Ref. 4)},\ h_o = \frac{1}{m_o}\sum_{n=1}^{\infty} m_n h_n. \qquad (6)$$

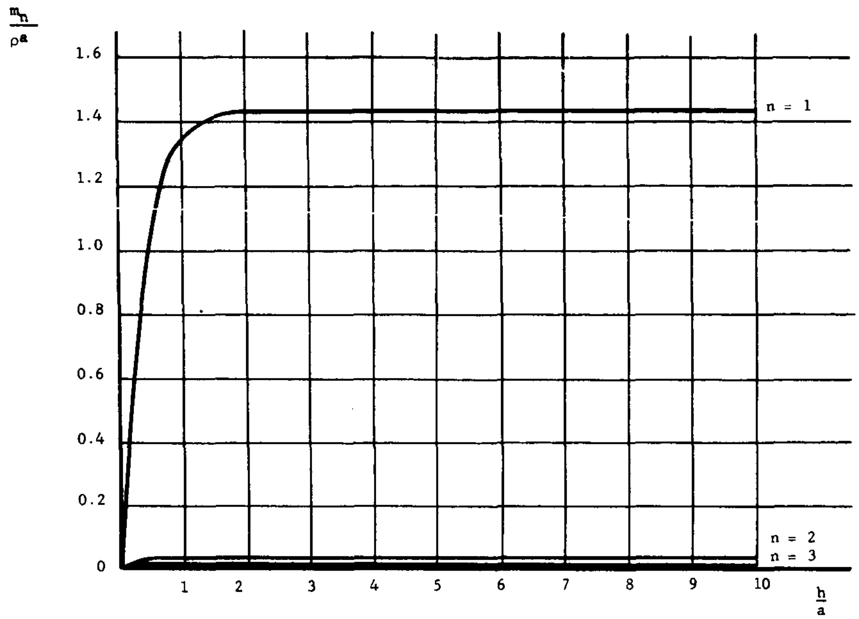

FIGURE 7. (U) SLOSHING MASS VERSUS FLUID HEIGHT RATIO

It can be seen that the absolute value of the sloshing mass is the same as long as the ratio $\frac{h}{a} > 2$. The first mode contributes the main part to the sloshing mass, while the second mode is below 3 percent of the first in a circular cylindrical tank, thus indicating that only the effect of the first mode need be considered in a stability analysis. The ratio of sloshing mass to total liquid mass increases greatly with decreasing fluid height, indicating that for short containers a large percentage of the liquid in the tank is sloshing. This is quite important for the design of the pressurization equipment. If a large mass ratio participates in the propellant motion, a mixing of cold layers with warm liquid layers occurs, thus cooling and condensing the pressurization gas, resulting in pressure loss. It is for this reason also that propellant sloshing should be suppressed (FIG. 8).

Of course, as can be imagined, pressurization can best be handled if there is no disturbance element (baffle) at all in the tank. This, however, holds only as long as the exciting frequency is not too close to the resonance frequency of the liquid because then the propellant is just slipping up and down the tank wall. Unfortunately, the forces and moments exerted by the propellant can be such that, from the dynamic

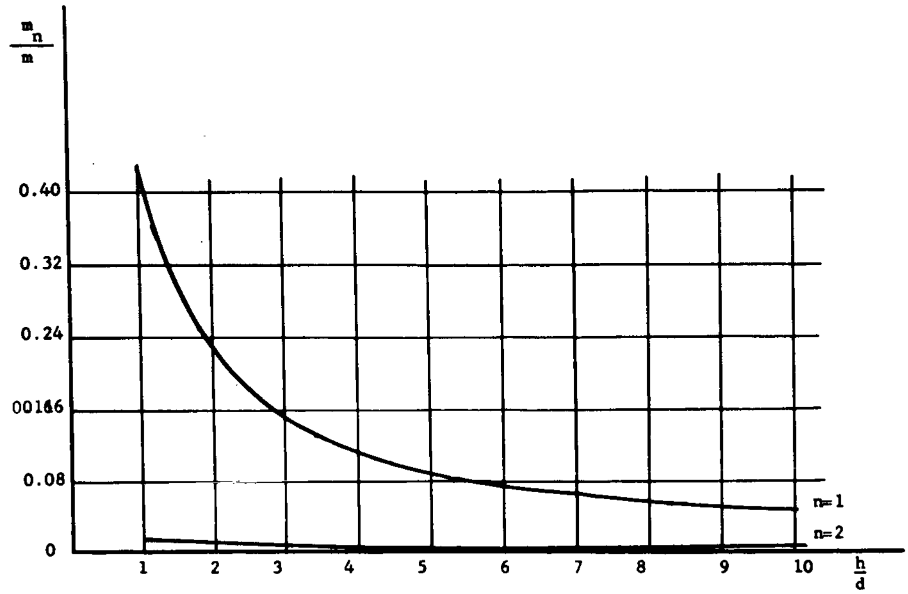

FIGURE 8. (U) SLOSH MASS RATIO VERSUS FLUID HEIGHT RATIO

standpoint, baffles have to be introduced to decrease the effect of the propellant motions upon the stability. These baffles again worsen the situation with respect to pressurization, since they disturb the flow field and create turbulence, which means a mixing of cold and warm layers of the cryogenics. Near resonance, however, the baffles usually suppress excessive spray, thus making pressurization less of a problem than without them.

It furthermore can be seen that the masses of the mechanical model m_n have to be attached close to the free fluid surface. This is even more true for those of higher sloshing modes. The disturbances due to higher sloshing modes stay very close to the free surface, and do not penetrate far into the liquid. With decreasing fluid height, the masses, m_n, approach the center of gravity of the liquid ($h_n \rightarrow o$). Damping is now introduced by adding to the masses, m_n, dampers attached to the tank wall and having a damping coefficient of $c_n/2$. Also, the disc is connected through a damper with the tank bottom. The values of the dashpots (c_n) are obtained by sloshing experiments, while the value of the dashpot (c_1, and I_1) is found by spring torsion tests of a completely filled and closed tank. Usually c_1 is so small that it can be neglected. For I_1, one can take then the value [4], as obtained from analytical treatment with ideal liquid [5].

The model describing the motion of the liquid due to roll oscillations about an axis parallel to the tanks can be obtained with the same model and is shown in FIGURE 9. The motion of the propellant in the four fuel and four LOX tanks is described by one mechanical model.

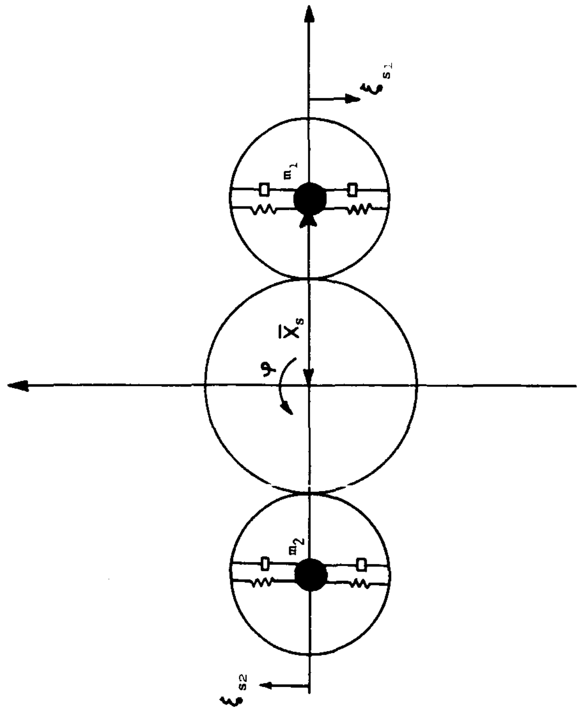

FIGURE 9. (U) ROLL SLOSH MODEL

In roll motion, the influence of the center tank, about which axis the motion takes place, can be neglected [6]. The moment of inertia of the liquid participating in the roll oscillation due to wall friction drops very rapidly with increasing frequency to zero and can be neglected. The roll damping, of course, increases with increasing roll exciting frequency.

It can now be concluded that clustering of the tanks is beneficial from the standpoint of propellant sloshing. The combined sloshing masses of booster tanks are only a fraction of that of two big diameter tandem tanks. For containers of the same diameter, the frequency of the liquids, compared to that of a single tank, is increased by the fourth root of the number of containers. The total sloshing mass reduces like the reciprocal square root of the container number. For simple stability investigations, a simplified system could therefore be treated, which considers the propellant oscillation being described by only one mechanical model having the mass of the combined sloshing masses of the propellant in the clustered tanks.

C. (U) U-TUBE EFFECT

Clustering of tanks, however, requires interconnection of the tanks for the exchange of propellant should an engine fail. This introduces an additional complication; a new U-tube mode. Fortunately, the frequency of this mode is very low; it is also strongly damped by the small interconnecting pipe diameter. For two tanks of different diameters connected by a pipeline of small diameter, in which laminar flow was assumed, the natural frequency and the logarithmic decrement were determined. The governing differential equation for the displacement, z_1, in the large tank with radius, R_1, is nonlinear and was solved with the perturbation method. From the solution shown in FIGURE 10, it can be seen that the natural frequency is very small and that, with increasing longitudinal acceleration of the vehicle (i.e., with increasing flight time), the frequency increases slightly. The growth

TANK SYSTEM

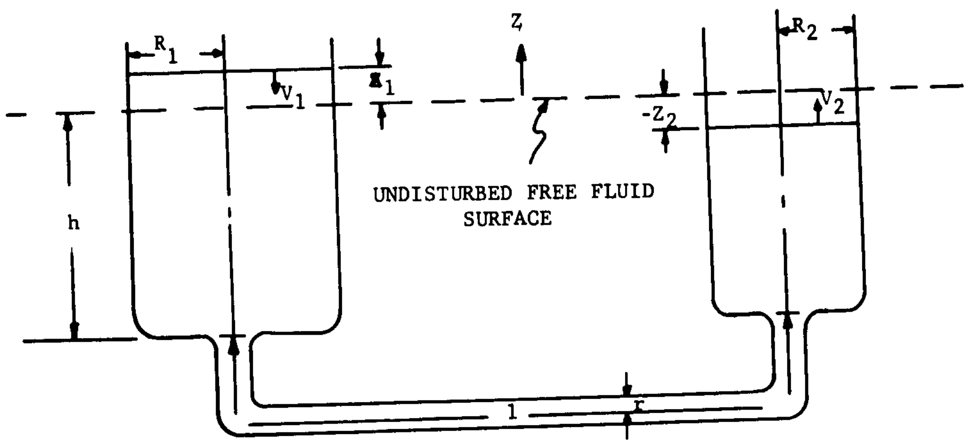

$$h\left[1+\frac{R_1^2}{R_2^2}\right]+\frac{lR_1^2}{r^2}+z_1\left[1-\frac{R_1^4}{R_2^4}\right]\ddot{z}_1+\frac{1}{2}\left[1-\frac{R_1^4}{R_2^4}\right]\dot{z}_1^2+\frac{8\nu l}{R_1^2}\dot{z}_1+g\left[1+\frac{R_1^2}{R_2^2}\right]z_1=0$$

$$f_o \approx \frac{1}{2\pi}\sqrt{\frac{g\left[1+\frac{R_1^2}{R_2^2}\right]}{h\left[1+\frac{R_1^2}{R_2^2}\right]+\frac{lR_1^2}{r^2}}}$$

$$\Delta \approx \frac{8\pi\nu l}{R_1^2\sqrt{g\left(1+\frac{R_1^2}{R_2^2}\right)\left[h\left(1+\frac{R_1^2}{R_2^2}\right)+\frac{lR_1^2}{r^2}\right]-\frac{16l^2\nu^2}{R_1^2}}}$$

FIGURE 10. (U) U-TUBE TANK SYSTEM

of the frequency is only slight, because the decreasing propellant height, h, partly cancels the effect of the acceleration, g. The logarithmic decrement decreases versus flight time, thus indicating that U-tube oscillations are likely to occur at a later flight time. However, the oscillations are strongly damped due to turbulent flow in the connecting small diameter pipeline and baffles in the tanks [7].

D. (U) EXPERIMENTAL RESULTS

As already mentioned, the damping of the propellant has to be obtained by experiments. The size of the Saturn, however, is such that full-scale tests would be time consuming and too expensive. Therefore, small laboratory models to simulate the liquid motion are used:

1. For the determination of approximate values for the equivalent damping of the liquid.

2. For the investigation of the effectiveness of various damping devices, their width, location, and geometry.

3. For the investigation of the effect of various parameters, such as viscosity, longitudinal acceleration, exciting amplitude, and tank geometry.

The damping characteristics of various damping devices are of particular importance, especially the effect of their configuration, width, and location. Since full-scale tests are expensive, and in many cases not possible, model tests are performed. Proper attention, however, must be given to the similitude relation; thus the model and the test liquid must be selected to insure dynamic similarity with the liquid propellants employed in the prototype vehicle [8].

The result of this analysis can be seen in FIGURE 11. For increasing equivalent Reynolds number, the damping decreases. This indicates that, for increasing acceleration, the efficiency of the damping devices decreases. Furthermore, it shows the loss of effectiveness of a certain baffle with increasing tank diameters.

A baffle should be located where the highest flow velocity appears; its direction should be perpendicular to the flow-velocity vector. For an annular ring baffle, this location would be at the tank wall where maximum upward and downward velocity occurs. For design reasons, this type of baffle is usually applied. A baffle located in the free-fluid surface would have the maximum damping effect if the amplitudes were infinitely small. For finite amplitudes, however, the efficiency of this baffle decreases considerably, since half of the baffle is always outside the liquid. The proper depth of the baffle below the free-fluid surface is dependent upon surface amplitude and tank form. Also the width of the baffle influences damping. For moderate amplitudes, the baffles should be located at a distance of about 0.08 radius under the free-fluid surface [9] for maximum efficiency (FIG. 12). Furthermore, the efficiency of the baffle drops very fast with increasing depth, indicating that, for a changing liquid level, another baffle should be located at a distance from the first baffle, so that the loss of efficiency of the first baffle is made up by the second, etc. Therefore, placing baffles 0.2 radius apart (instead of 0.4 radius as shown in FIGURE 13 should provide a relatively constant damping factor.

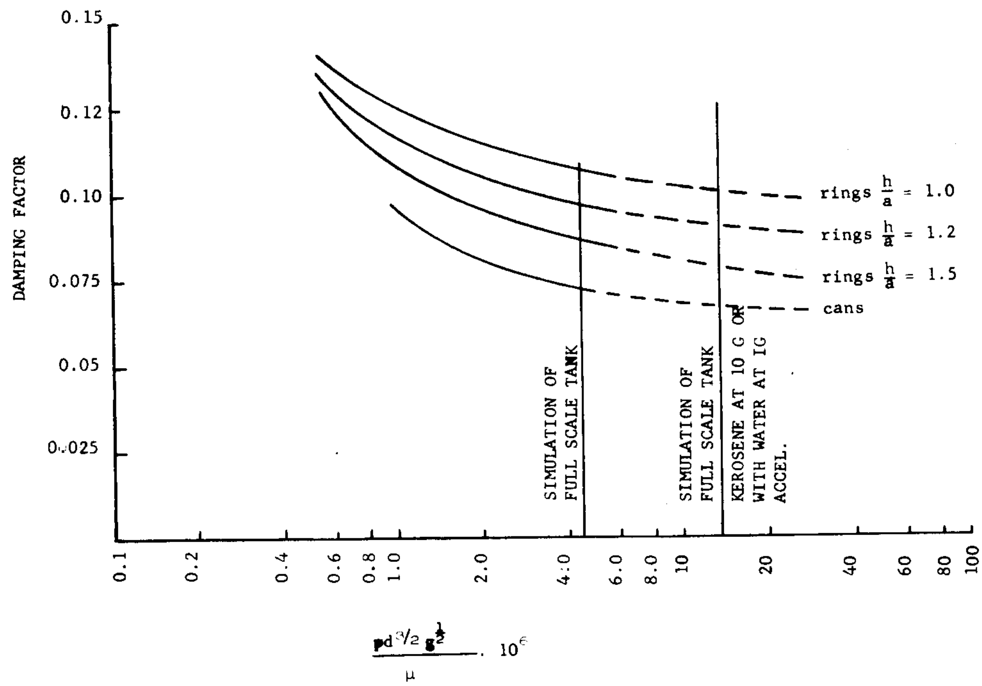

FIGURE 11. (U) INFLUENCE OF ACCELERATION, VISCOSITY, AND TANK DIAMETER ON THE SLOSH DAMPING FACTOR

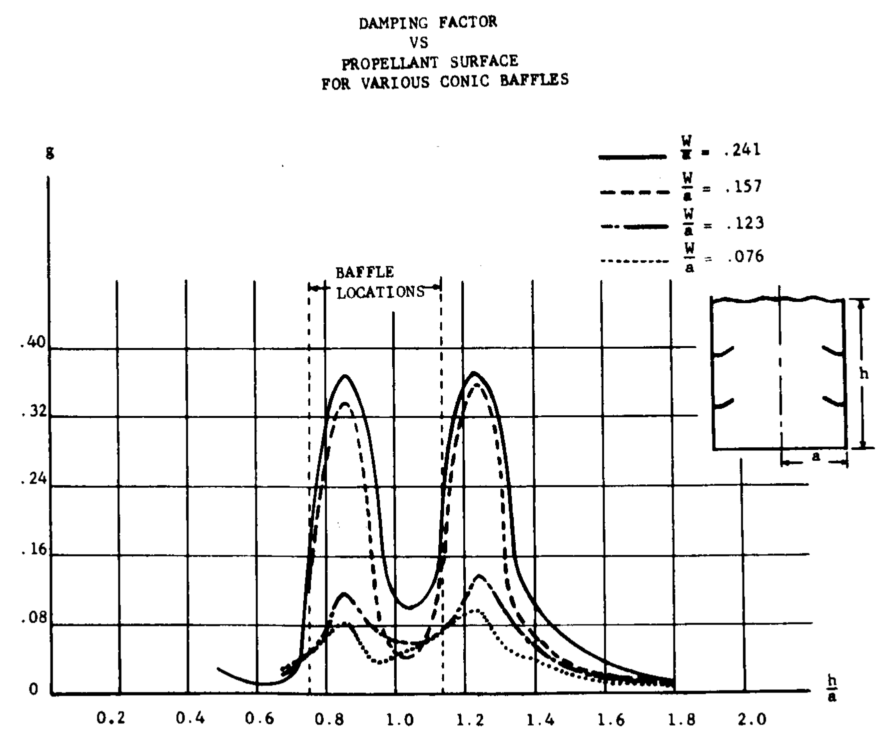

FIGURE 12. (U) VARIATION OF THE DAMPING FACTOR WITH BAFFLE LOCATION

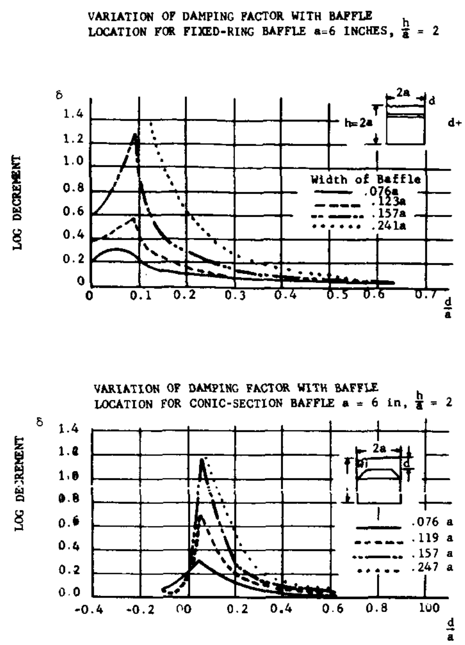

FIGURE 13. (U) DAMPING FACTOR VERSUS PROPELLANT SURFACE FOR VARIOUS CONIC BAFFLES

E. (U) VORTEX PREVENTION IN THE TANKS.

Another problem is the formation of a vortex in emptying tanks because it reduces the propellant flow rate due to the reduction of the effective cross section of the drain outlet and can lead to pump cavitation toward the end of flight time. This indicates that excess propellant must be carried and that at cutoff a large residue remains unused in the tanks. This residual propellant can be in appreciable amounts thus reducing the performance of the vehicle. Comparatively little is known about vortex formation because of the difficulties in analytical treatment. Therefore, most of the work is of a qualitative nature and is based on visual or photographic studies. The formation of a vortex during draining of the tank depends upon the amount of initial rotation of the liquid and the fluid height. There are, fortunately, a number of factors which help prevent the vortex formation. First, sloshing itself tends to break up the surface and moves the liquid across the tank, thus disturbing the vortex. Second, the baffles, which help prevent the regular sloshing, help create some disturbance, and third, the application of anti-vortex baffles such as a cross at the drain outlet and a flat plate above the outlet. The latter one forces the vortex around its surface, thus preventing its formation in full magnitude, while the first one prevents rotation.

A series of model tests have been performed to find out which device would best prevent vortexing even with prerotation of the liquid. This device, consisting of sexpartite cross with a 20-mesh screen of hemispherical slope on top, was mounted in the discharge line.

During tests, it was detected that, due to the interconnection of tanks, a surge problem occurred in the outer tanks, which was caused by the flow from the interconnecting line from the center tank. This behavior was remedied by elongating the suction line into the fuel tank and putting a "Chinese Hat" above the outlet of this pipe.

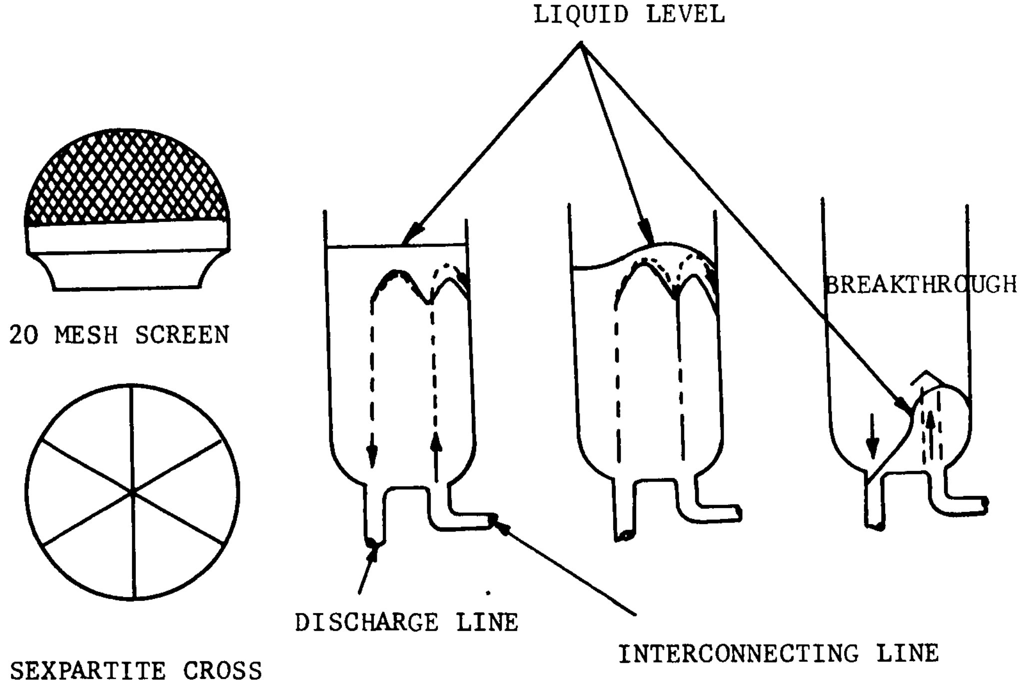

FIGURE 14. (U) ANTI-VORTEX DEVICE AND "CHINESE HAT" FOR THE PREVENTION OF THE SURGE PROBLEM

F. (U) SIMPLIFIED STABILITY BOUNDARIES.

To efficiently study the influence of the propellant sloshing upon the stability of the vehicle and still indicate proper trends, the sloshing in the booster tanks is described by one mechanical model. Very useful general results can be obtained from these simplified stability investigations. Due to the low bending frequency, the influence of the elastic behavior must be taken into consideration. A parametric study investigates the possibility of eliminating instabilities due to propellant motion in the tanks of the vehicle. There are several methods to eliminate the effect of the propellant sloshing upon the stability to a great extent. Some methods are:

1. Tank geometry

2. Tank location

3. Choice of the control system

4. Introduction of mechanical baffles

The influence of tank geometry, i.e., the clustered tanks in the case of the SA-1 vehicle, has already been mentioned as being beneficial, since it reduced the sloshing mass and increased the natural frequency of the liquid. The tank locations are usually given and can only be exchanged with other tanks. An exchange of heavy liquid oxygen with light liquid hydrogen can result in better stability. In the SA-1, the tank locations were given. A third means of suppressing the control hazard due to propellant sloshing is the proper selection of the type, location, gain values, and vibrational characteristic of the control sensors. Since baffles mean an additional weight penalty, they are employed only as a last resort. The influence of the various parameters is expressed by stability boundaries, which are determined in terms of the amount of damping of the propellant in the tank required for various tank locations (slosh mass location). It was found [10]that the control frequency should be below the sloshing frequency to avoid unnecessary bottling in the tanks (FIG. 15).

STABILITY BOUNDARY FOR RIGID SPACECRAFT
(NO ADDITIONAL CONTROL)

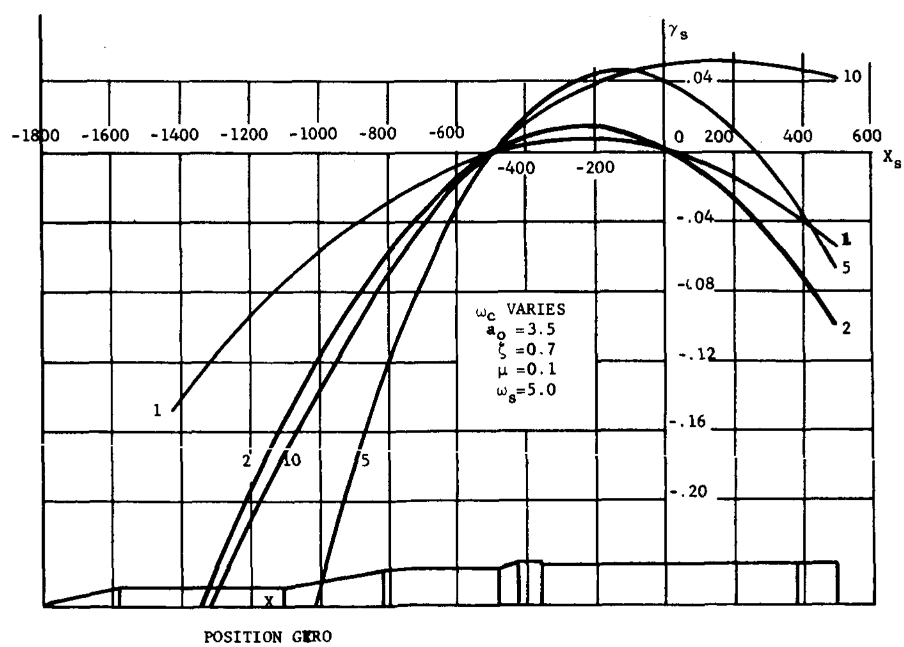

FIGURE 15. (U) STABILITY BOUNDARY FOR RIGID SPACECRAFT

The danger zone where instability due to propellant sloshing, may occur, if not properly damped, lies between the center of gravity and the center of instantaneous rotation and can be enlarged especially toward the rear of the vehicle by the elastic behavior of the vehicle [11]. This demands more and stronger baffling. The change of the control damping, ζ_c, exhibits the following trend: For increasing subcritical control damping ($\zeta_c < 1$), the stability decreases in the danger zone; i.e., more damping has to be introduced to maintain stability. For increasing super-critical control damping ($\zeta_c > 1$), the stability increases. From these considerations it is concluded that the Saturn booster tanks should be baffled with perforated accordion baffles in the upper half (FIG. 16). Due to the lower natural frequency of the propellant in the inner tanks, a damping in this tank should be maintained during the complete flight time. The center tank, therefore, was baffled along its entire length with accordion baffles (FIG. 17).

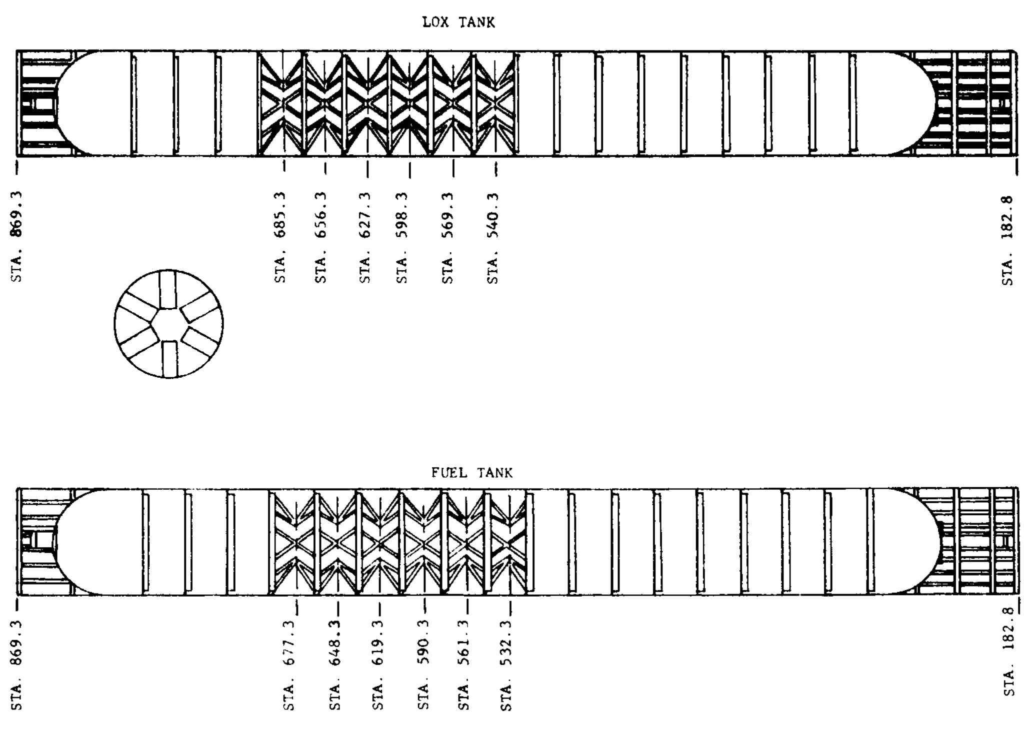

BAFFLING OF 70" LOX AND FUEL TANKS

FIGURE 16. (U) BAFFLING OF OUTER CONTAINERS

G. (C) OVER-ALL FEEDBACK ANALYSIS.

It is assumed that the motion of the SA-1 vehicle can be described by the superposition of a finite number of pre-assigned mode shapes together with the translation, rolling, and pitching of the airframe of the vehicle. The motion of the engine relative to the

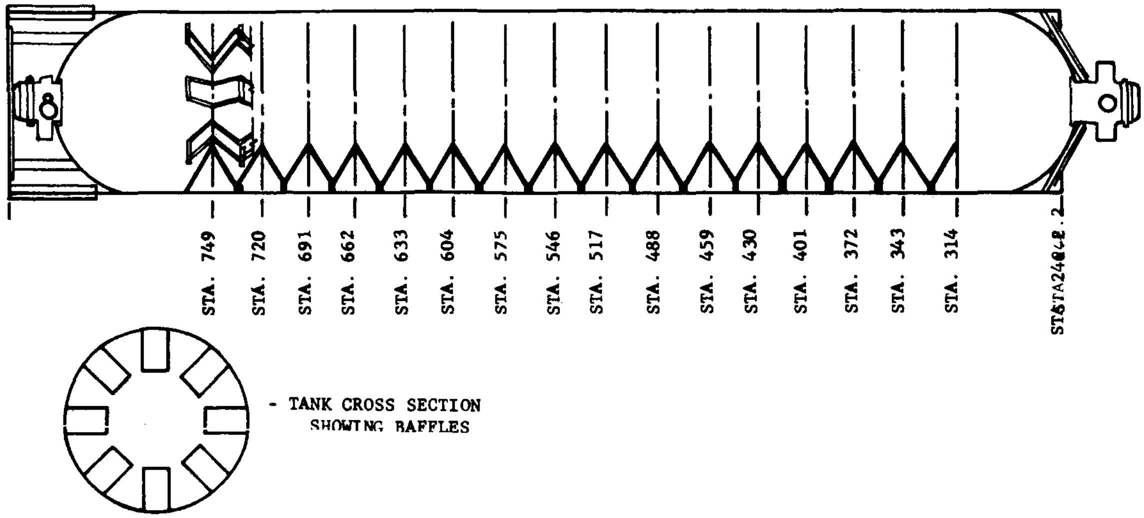

FIGURE 17. (U) BAFFLING OF CENTER CONTAINER

inertial system and the motion of the propellant, being described by the mechanical model, are also considered. Three models were used to describe the motion of the propellant: One model for the LOX in the center tank and one model each for the four fuel outer tanks and four LOX outer tanks. The sloshing masses versus flight time are given in FIGURE 18. It can be seen that the sloshing mass ratio increases with flight time.

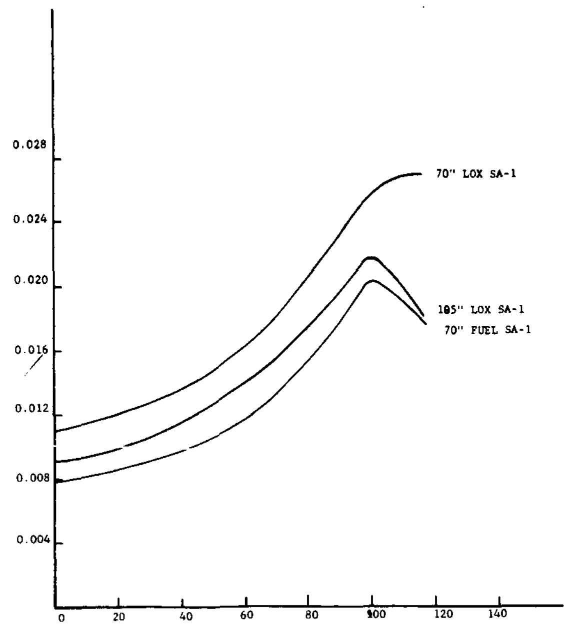

FIGURE 18. (U) RATIO OF SLOSHING MASS TO TOTAL VEHICLE MASS VERSUS FLIGHT TIME

The absolute sloshing mass stays constant during most of the flight time and decreases at the end of the burning time due to the change of the tank diameter.

The compliance of the swivel engines, i.e., the difference (β_c - β_E) between the actual deflection angle, β_E, and the control signal, β_c, is also introduced. After the determination of the kinetic and potential energy, as well as the dissipation function and the reaction moments in the gimbaling points of the engines, the equations of motion can be found applying the Lagrange equation in a modified form for the various generalized coordinates. The generalized forces result from thrust, aerodynamic forces, and drag, and even forces of the flowing propellant. The control system of SA-1 consisted of an attitude channel with a differentiating (lead) network to provide sufficient damping for the stabilization of the system. In addition to this, local angle-of-attack meter control was used.

The theoretical analysis consists now in solving this system of differential equations under the assumption of a time dependency, e^{st}, of all generalized coordinates. This provides us with the roots $s = \sigma + i\omega$ of the system, some of which are stable and some unstable. Introducing now a deliberate variable-phase angle permits the determination of optimum stability; performing this for the various modes and flight times results in a phase requirement that has to be met by the hardware design of shaping network. A fair representation of the optimum network was used in the flight.

It was found that the roots connected with the propellant were stable with the introduced baffles (FIG. 19 and 20). Since the accordion baffles provide a damping factor between $0.05 \leq \zeta \leq 0.06$, the sloshing roots in the center tanks exhibit good stability. The same can be observed in the outer tanks. The discontinuity in the roots at 90 seconds flight time is due to a capacitor switching, which brings the control damping back to its nominal value of $\zeta_c = 0.7$, thus increasing the stability. The stability in the outer tanks becomes marginal, since at the end of powered flight time, the damping value of the slosh damping factor varies between 0.01 and 0.03, depending, of course, upon the location of the stiffener rings with respect to the free-fluid surface.

The roots due to sloshing propellant in roll were all stable with the originally anticipated roll control system.

[redacted]

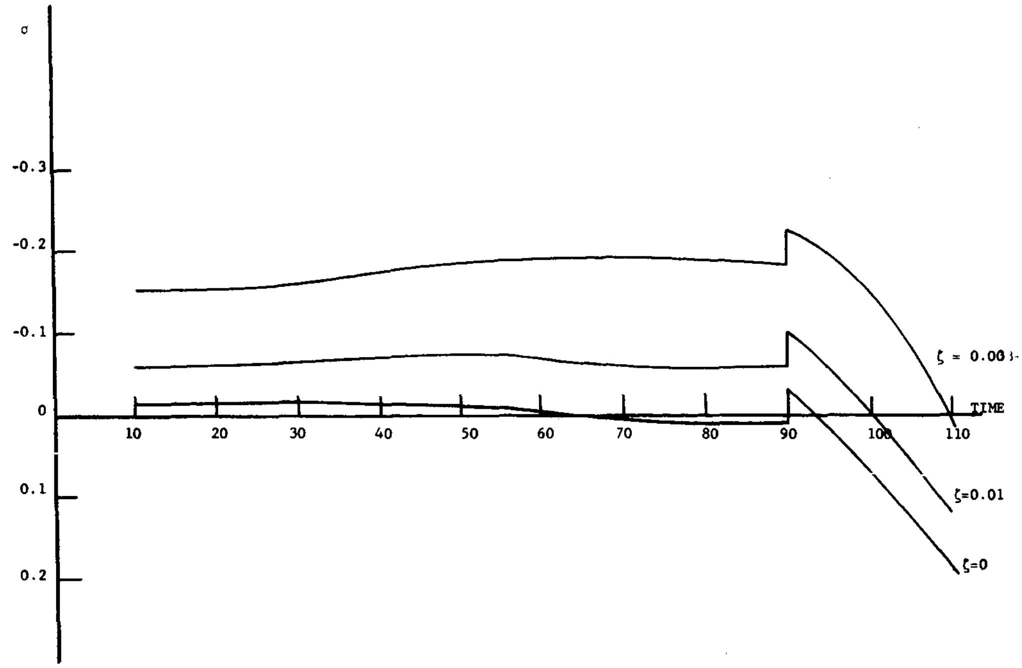

FIGURE 19. (U) ROOTS OF THE PROPELLANT IN THE CENTER TANK FOR VARIOUS SLOSH DAMPING FACTORS (PITCH AND YAW)

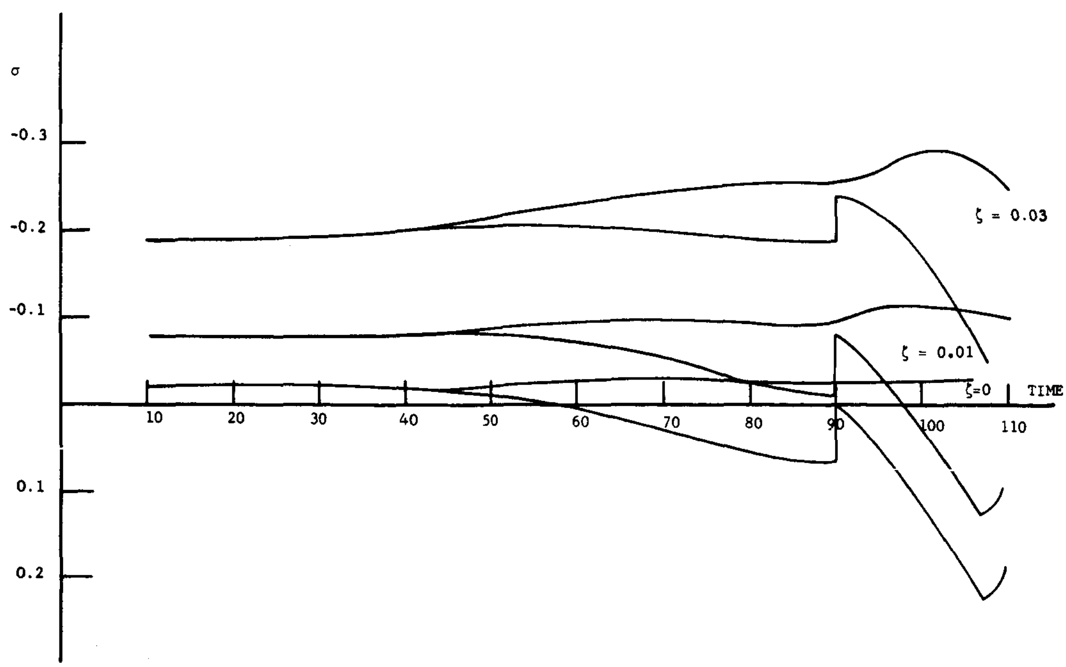

FIGURE 20. (U) ROOTS OF THE PROPELLANT IN THE OUTER TANKS FOR VARIOUS SLOSH DAMPING FACTORS (PITCH AND YAW)

[redacted]

H. (C) FLIGHT RESULTS.

Pressure difference sloshing measurements have been performed with potentiometer-type differential transducers in three of the nine tanks. The center tank, one fuel tank, and one LOX outer tank, were equipped with measuring devices. The range of these measurements was exceeded at 109 seconds after liftoff.

Right after liftoff, a small roll oscillation occurred, but was completely damped out after five seconds. At that flight time, enough damping is provided so that the propellant in the tanks does not further increase the roll amplitude by propellant sloshing. Furthermore, enough lead in the roll loop is provided for stability. See FIGURE 21 at about 0.8 cps (old filter).

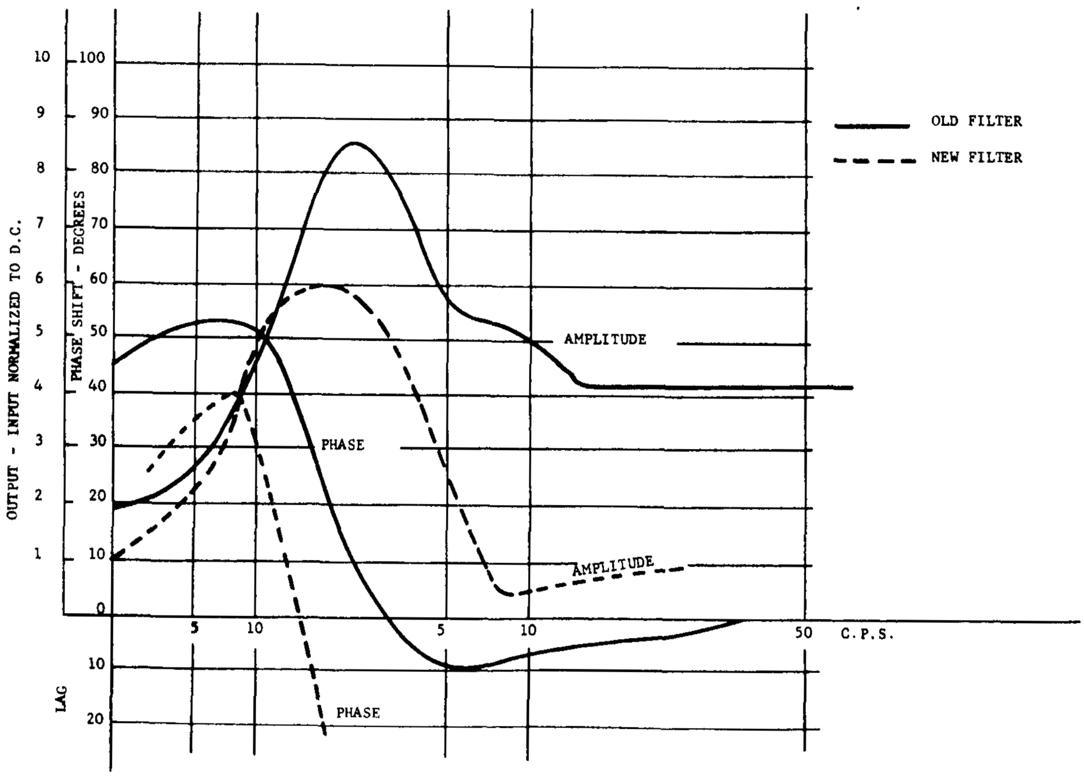

FIGURE 21. (U) FILTER RESPONSE CURVES OF THE LEAD NETWORK IN ROLL

In pitch and yaw, no instability occurred due to sloshing propellant until 94 seconds flight time. In the center tank, an oscillation with increasing amplitude occurred after the propellant level passed below the last baffle. Here the damping factor of $\zeta = 0.06$ provided by the accordion baffles drops down to the smooth wall value of $\zeta = 0.005$ to 0.01. The theoretical analysis (FIG. 19) shows that for a propellant damping factor between $\zeta = 0.005$ and $\zeta = 0.01$ instability occurs between 86 and about 104 seconds flight time. This slight instability, however, is harmless from the dynamic standpoint. It will, unfortunately, aggravate the pressurization of the LOX tank and can also lead to premature cutoff.

At about 90 seconds flight time, a divergent roll oscillation with an average frequency of about 1.5 cps was excited by the propellant sloshing in roll. Due to the relatively long lever arm (FIG. 9) of the sloshing masses from the center-line of the vehicle, the torque on the vehicle is considerable. This instability was essentially the result of an incompatibility of the filter network in the roll control loop. The original design of the roll control filter, however, was thoroughly investigated with respect to propellant sloshing and was found to maintain stability for the vehicle. Later, uncertainties in the torsional model arose from the comparison of test results from the SA-D dynamic tests with the theoretical values. Two close torsion frequencies appeared, one of which could not be predicted by theoretical means. As a result, a last-minute change introduced a stronger attenuation applied already at a smaller frequency, which also resulted in a stronger phase lag. This covered the uncertainties with respect to the torsional modes, thus stabilizing all torsional modes by attenuation stabilization. FIGURE 21 exhibits the response curves of the lead network filter. The dashed lines are the amplitude and phase of the changed filter. It can be seen that, to accomplish this attenuation at 4 cps and above, there appears an inherent phase lag in the loop. This phase lag crosses the frequency axis at about 1.5 cps and leads to the sloshing instability. At flight time between 90 seconds and 100 seconds, the natural frequency in the outer tanks is about 1.4 cps. Time did not permit a study of the influence of this change upon sloshing. At 102.8 seconds, the motion in the tanks changed from a linear to a rotary motion, which continued until the loss of the measurements. The sloshing in the tanks and probably the rotary motion of the liquid in the containers contributed about one-half to the premature cutoff of 1.61 seconds of the inner engines [12]. The cutoff sensor, which triggered the earlier cutoff, was located in a fuel tank at about 19.5 inches from the center of this tank. The sloshing amplitude of about 5 inches was necessary to give the signal for cutoff. After cutoff of the inner engines, the propellant sloshing died immediately, since its natural frequency was due to half the longitudinal acceleration reduced by a factor of $\sqrt{2}$. Thus, the first natural frequency in the outer tanks dropped from 1.4 cps to about 1.0 cps at which the filter provided enough lead for stability.

The rotational type of liquid motion appears during the regular sloshing as soon as the forcing frequency approaches the resonance frequency of the liquid. It is probably best described as an apparent "rotation" of the liquid about its vertical axis of symmetry; i.e.,

[redacted]

the nodal line of the free-fluid surface is rotating about the longitudinal axis. The motion is similar to that of a spherical pendulum, the suspension point of which is excited at a certain frequency. It may be noted that that this type of motion also appears in a rectangular tank. The motion is even more complicated since a type of "beating" also seems to exist; i.e., near slosh resonance, the nodal line of the free-fluid surface starts to rotate in a certain direction, reaches a maximum, decreases until it is at rest, and then reverses its direction of rotation, and so on, alternately. The baffles used for the suppression of the regular sloshing motion also greatly help to prevent this type of rotation.

In FIGURES 22 and 23, the roots of the propellant in the outer tanks are given (for the filter used in flight) for various propellant slosh damping factors. It can be seen that the roots corresponding to the propellant motion out of phase with the excitation are all stable with wall friction, while those wherein the propellant motion is in phase with the excitation are at the end of powered flight time very instable. The value of the damping factor, of course, varies between $\zeta = 0.005$ and $\zeta = 0.02$, depending on the location of the stiffener rings in the tanks. In the fuel tanks, the last stiffener ring was located where the propellant surface passed through at about 100 seconds. From FIGURE 13, it can be seen that the damping factor decreases very rapidly with increasing

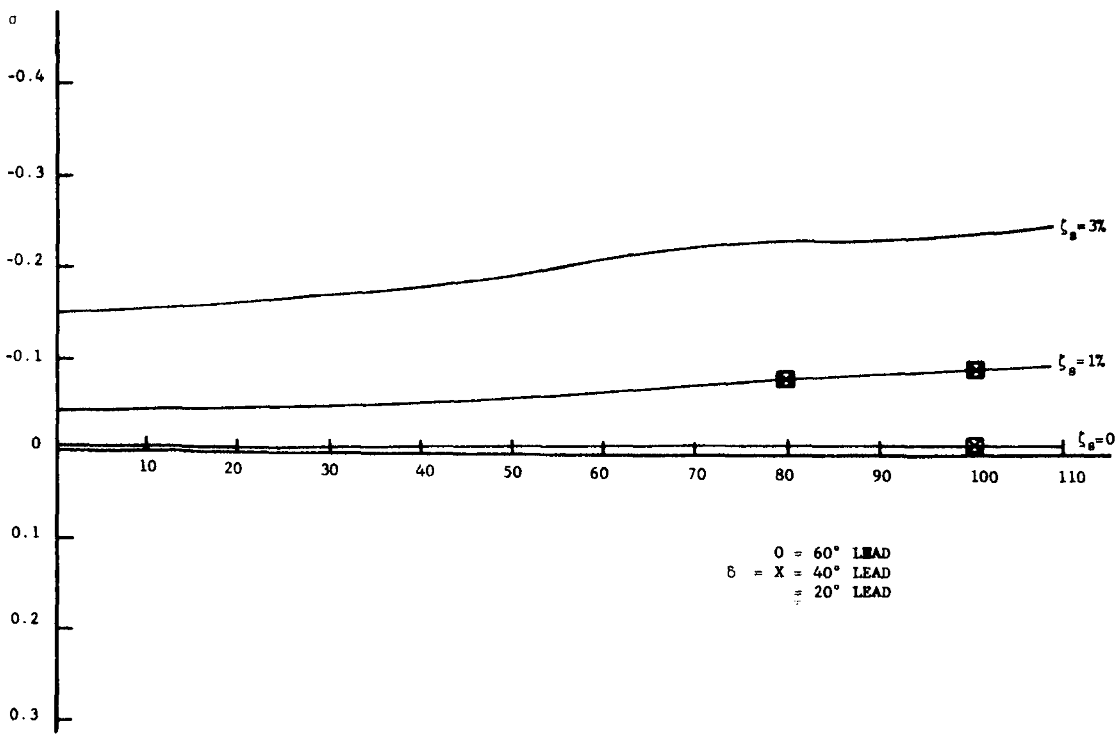

FIGURE 22. (U) ROOTS (OUT OF PHASE) OF THE PROPELLANT IN THE OUTER TANKS FOR VARIOUS SLOSH DAMPING FACTORS (ROLL)

[redacted]

[redacted]

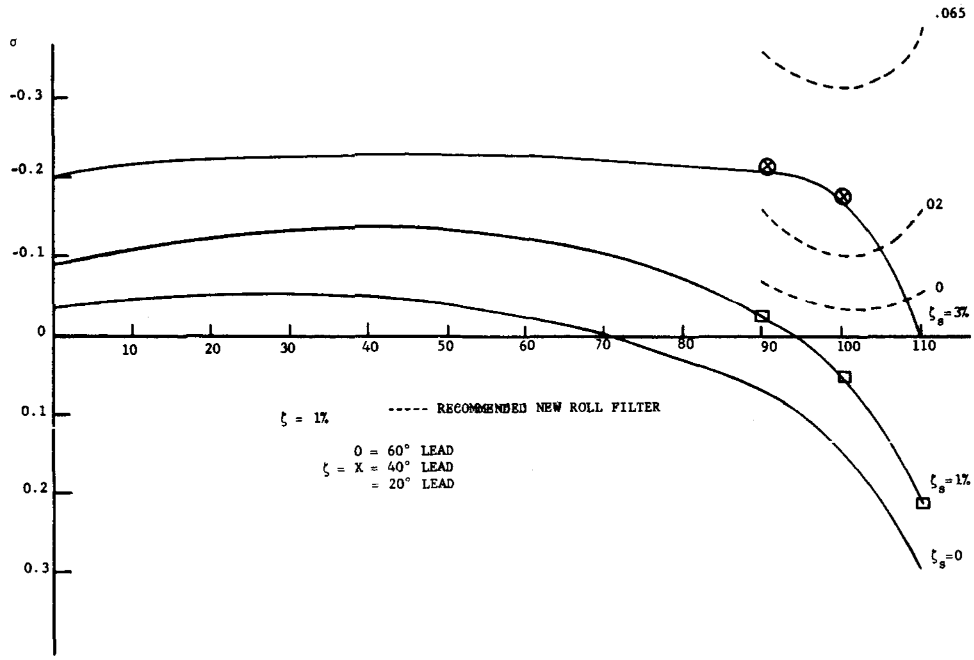

FIGURE 23. (U) ROOTS (IN PHASE) OF THE PROPELLANT IN THE OUTER TANKS FOR VARIOUS SLOSH DAMPING FACTORS (ROLL)

depth of the baffle below the free propellant surface. It, furthermore, exhibits that, after the liquid surface passed through its optimum position with respect to the baffles damping factor, the efficiency of the baffle decreases considerably. Telemeter measurements indicated clearly that, shortly before the stiffener ring left the free propellant surface, the sloshing amplitude increased considerably. In FIGURE 23, it can be seen that, for a propellant damping factor of about $\zeta = 0.01$, instability occurs at about 95 seconds. This instability increases with increasing flight time. This is in agreement with the actual flight results.

SECTION IV. (C) CONCLUSION

For reasons of sloshing stability at the end of the powered flight of future Saturn vehicles, it was decided to include a set of accordion baffles for all remaining Block I vehicles covering the last three stiffener rings in the LOX tank and a set of three accordion baffles covering the last three rings in the fuel tank. This could be sufficient to maintain appropriate stability up to the powered flight time of about 102 seconds. From that time on, only wall friction is available and sloshing, therefore, could build up to create again instability of the vehicle. Furthermore, the formation of a vortex and especially the rotary motion of the propellant can be excited during the last few seconds of powered flight time. Especially, for later vehicles, where

[redacted]

a separation procedure follows after cutoff, the stability of the vehicle in these last seconds of first stage powered flight is of great importance. These effects can be prevented and the regular sloshing in the lower part of the tanks can be suppressed by the application of a cross device at the tank bottom. This device would prevent vortex formation as well as the rotary motion of the liquid. This would prevent premature cutoff. It furthermore would increase the natural frequency of the propellant by a factor of about 1.4 and would also considerably decrease the sloshing mass, which will produce the main effect upon the stability. The mass of the sloshing propellant will be reduced by the cross device by more than 50 percent. In addition to the baffles included in Block I vehicles, a cross device will be introduced at the tank bottom in Block II vehicles. Furthermore, as indicated in FIGURE 23, the lead network of the roll channel should be changed, thus giving better stability at the critical powered flight time, as is indicated by the dotted line. This can be performed without endangering the torsional stability.

(U) REFERENCES

1. H.F. Bauer, "Fluid Oscillations in a Circular Cylindrical Tank, ABMA Report DA-TR-1-58, May 16, 1958.

2. H.F. Bauer, "Propellant Oscillations in Cylindrical Tanks."

3. H.F. Bauer, "Fluid Oscillations in a Cylindrical Tank with Damping," ABMA DA-TR-4-58, April 23, 1958.

4. H.F. Bauer, "Mechanical Analogy of Fluid Oscillations in Cylindrical Tanks with Circular and Annular Cross Sections," MSFC, MTP-AERO-61-4, January 12, 1961.

5. H.F. Bauer, "Moment of Inertia of a Liquid in a Circular Cylindrical Tank," ABMA Report DA-TR-5-58, April 23, 1958.

6. H.F. Bauer, "The Effective Moment of Inertia in Roll of Propellant and Roll Damping," ABMA Report DA-TM-67-59, May 26, 1959.

7. H.F. Bauer, "Damped Oscillations in a Connected Fluid System," ABMA Report DA-TM-57-59, May 1, 1959.

8. H.N. Abramson, G.E. Ransleben, Jr., "Simulation of Fuel Sloshing Characteristics in Missile Tanks by Use of Small Models, ARS Journal, July 1960.

9. D.G. Stephens, M.A. Silveira, H.W. Leonard, "An Investigation of the Damping of Liquid Oscillations in Cylindrical Tanks Fitted with Various Types of Baffles," NASA TN-D-715, 1961.

10. H.F. Bauer, "The Effect of Propellant Sloshing on the Stability of an Accelerometer Controlled Rigid Space Vehicle," MSFC, MTP-AERO-61-16, March 6, 1961.

11. H.F. Bauer, "Stability Boundaries of a Liquid Propelled Elastic Spacecraft," MSFC, MTP-AERO-61-7, February 7, 1961.

12. F. Speer, "SA-1 Flight Evaluation," MSFC, MPR-SAT-WF-61-8, December 14, 1961, Confidential.

(U) APPROVAL MTP-AERO-62-29

PROPELLANT SLOSHING PROBLEMS OF SATURN

By Helmut F. Bauer

The information in this report has been reviewed for security classification. Review of any information concerning Department of Defense or Atomic Energy Commission programs has been made by the MSFC Security Classification Officer. The highest classification has been determined to be Confidential.

Helmut F. Bauer

Helmut F. Bauer
Chief, Flutter and Vibrations Section

H. Horn

Helmut J. Horn
Chief, Dynamics Analysis Branch

Geissler

E.D. Geissler
Director, Aeroballistics Division

(U) DISTRIBUTION

INTERNAL

Director, MSFC
Deputy Director, MSFC

Saturn Systems Office
Dr. O. H. Lange

Computation Division
Dr. Hoelzer
Dr. Fehlberg
Dr. Schulz-Arenstorff
Miss Morgan

Manufacturing Engineering Division
Director
Deputy Director
Mr. H. Wuenscher

Astrionics Division
Director
Mr. Hosenthien
Mr. B. Moore
Mr. Digesu

Launch Operations Directorate
Director
Dep Director
Dr. A. H. Knothe

Research Projects Division
Director
Mr. Miles
Mr. J. Dowdy

Test Division
Director
Dep Director
Dr. Sieber
Mr. Haukohl
Mr. Schuler

(U) DISTRIBUTION (CONT'D)

Propulsion and Vehicle Engineering Division

Director
Dep Director
Mr. Hellebrand
Mr. Kroll
Mr. Paul
Mr. Palaoro
Mr. Heusinger
Mr. Schulze
Mr. M. Nein
Mr. Hunt
Mr. Voss
Mr. Bergeler
Mr. Neighbors
Mr. Goerner
Mr. Engler

Aeroballistics Division

Director
Dep Director
Mr. Horn
Mr. Dahm
Mr. Reed
Dr. Speer
Mr. Rheinfurth
Mr. Ryan
Mr. Hart
Mr. Golmon
Mr. Stone
Mr. Baker
Mrs. Chandler
Mr. Larsen
Mr. Beard
Mr. Pack
Mr. Kiefling
Mr. Bauer
Dr. Sperling
Mr. Hays
Mr. Franke
Mr. Wells
Mr. Thomae
Mr. Vaughan
Mr. Scoggins
Mr. Payne

M-MS-IP M-HME-P

M-MS-IPL (8)

M-PAT

M-MS-H